Next-generation sequencing elucidates the distinct mutational landscape of SMARCA4-deficient lung cancer

FEICHENG YANG[1], YUZHONG YANG[2], ZHIHONG CHEN[1], YANCHUN LI[1] and YINGHUI SONG[3]

[1]Department of Pathology, Hunan Provincial People's Hospital and The First Affiliated Hospital of Hunan Normal University, Changsha, Hunan 410005, P.R China; [2]Department of Pathology, Guilin Medical University Affiliated Hospital, Guilin, Guangxi Zhuang Autonomous Region 541001, P.R. China; [3]Central Laboratory, Hunan Provincial People's Hospital and The First Affiliated Hospital of Hunan Normal University, Changsha, Hunan 410005, P.R. China

Received July 22, 2025; Accepted February 11, 2026

DOI: 10.3892/ol.2026.15636

Abstract. Lung cancer with SMARCA4 deficiency has a high degree of malignancy and a low degree of differentiation. It is a newly discovered type of tumor closely related to gene mutations. The present study aimed to clarify the molecular mutation characteristics of *SMARCA4*-deficient lung cancer using next-generation sequencing (NGS). NGS sequencing was conducted to analyze the gene expression profile of 15 patients with *SMARCA4*-deficient lung cancer, with positive or negative EGFR expression, and the association between gene mutation sites and *SMARCA4* expression was analyzed. The pathological characteristics of *SMARCA4*-deficient lung cancer were analyzed using immunohistochemistry. The likelihood of positivity for the programmed cell death 1 ligand 1 protein was low, and there were no instances of positivity for anaplastic lymphoma kinase protein expression. Approximately 50% of Ki67-positive expression regions were present. The BOI-related E3 ubiquitin-protein ligase 1 protein encoded by the *SMARCA4* gene was not expressed; however, the INI1 protein encoded by *SMARCB1* was partially positive (6/15), which showed that the expression of INI1 was not affected by *SMARCA4*. The *SMARCA4* mutation types included c.2729C>T (p.T910M), c.3634_3636del (p.E1212del), c.3574C>T (p.R1192C), and c.3733G>A (p.A1245T). *NQO1* and *TP53* mutations were detected in nine patients, *XRCC1* mutation was detected in seven patients, *DPYD* mutation was detected in six patients and *TYMS* mutation was detected in five patients. The mutated genes were more resistant to the EGFR tyrosine kinase inhibitor. In conclusion, patients with *SMARCA4*-deficient lung cancer have distinct immunohistochemical characteristics, and *SMARCA4* has been implicated in the incidence and progression of tumors through different mutation mechanisms.

Correspondence to: Professor Yanchun Li, Department of Pathology, Hunan Provincial People's Hospital and The First Affiliated Hospital of Hunan Normal University, 61 Jiefang Road, Changsha, Hunan 410005, P.R China
E-mail: lychglx@163.com

Professor Yinghui Song, Central Laboratory, Hunan Provincial People's Hospital and The First Affiliated Hospital of Hunan Normal University, 61 Jiefang Road, Changsha, Hunan 410005, P.R. China
E-mail: songyinghui@hunnu.edu.cn

Key words: SMARCA4, lung cancer, mutation, next generation sequencing, TP53

Introduction

As a crucial component of the SWI/SNF chromatin remodeling complex, *SMARCA4* modifies DNA histone interactions inside the nucleus to perform chromatin remodeling and regulate gene transcription (1). This complex largely influences various physiological and pathological processes, including brain development and cancer onset (2). *SMARCA4* regulates the CREST-BOI-related E3 ubiquitin-protein ligase 1 (BRG1) complex and neuron-specific gene expression in brain development; it contributes to the self-renewal and differentiation of neural stem cells (3). Additionally, *SMARCA4* co-regulates the transcription of E-cadherin with ZEB1 and is involved in the epithelial-mesenchymal transition (EMT) process (4).

Drug resistance and tumor progression are related to *SMARCA4* deletion or mutation, which are prevalent in various tumors, such as lung cancer and liver cancer (5,6). Approximately 20% of cancers include mutations in the SWI/SNF complex, and chromatin remodeling has substantial uses in tumor treatment. A synthetic lethal therapeutic technique based on the deletion of *SMARCA4* and *ARID1A* double alleles, a frequent type of mutation in SWI/SNF complexes, can kill tumor cells by targeting cancer cell-specific dependent subunits, such as *SMARCA2* or *ARID1B* (7). Additionally, some drugs that target SWI/SNF subunits have already been approved by the FDA and are undergoing clinical trials (8).

Through various mechanisms, including interferon signaling, DNA damage and mismatch repair and oncogene programmed regulation, SWI/SNF complexes can control the tumor immune microenvironment, thus improving the efficacy of immunotherapy (9). Changes in the subunit composition of the SWI/SNF complex control drug resistance and its progression in tumors. For *SMARCB1* mutant cancers, the influence of DCAF5's quality control on SWI/SNF complexes may be

a therapeutic target (9-11). Additionally, through controlling gene transcription, SWI/SNF complexes contribute to cell differentiation and tumor suppression (11).

The microbiome and microbial extracellular vesicles are becoming increasingly important in the pathophysiology of lung cancer and therapeutic strategies (10). Lung cancer detection and treatment have also benefited from the advancement of molecular pathological diagnosis (11). *SMARCA4*-deficient non-small cell lung cancer (*SMARCA4*-dNSCLC) is a malignant tumor with poor differentiation (12). Surgery is the primary course of treatment, and some patients may require adjuvant chemotherapy or immunotherapy after surgery (13). *SMARCA4*-dNSCLC has an unfavorable prognosis, with a median survival period of ~12.2 months (14). This necessitates a thorough examination at the genetic and molecular levels in clinical practice because of the paucity of research on the pathophysiology and clinical features of this malignancy. The present study primarily used pathological morphology and molecular genetic diagnosis to analyze the disease characteristics of *SMARCA4*-dNSCLC. Using second-generation sequencing technology, the genetic polymorphism of SMARCA4 in lung cancer was examined, yielding important knowledge for clinical diagnosis and treatment.

Materials and methods

Patient data. This study included 15 patients with SMARCA4 mutations. The study retrospectively investigated patients who underwent high-throughput lung cancer sequencing in the Pathology Department of Hunan Provincial People's Hospital (Changsha, China) from January 2021 to November 2024. Among them, there were 9 male patients and 6 female patients, with an age range of 34 to 84 years, and an average age of 60.5 years. The inclusion criteria for the study subjects are as follows: i) Patients who underwent high-throughput lung cancer sequencing in the Pathology Department of Hunan Provincial People's Hospital (Changsha, China) from January 2021 to November 2024; ii) patients diagnosed with lung cancer through histopathology or cytology; iii) patients whose high-throughput sequencing results indicated SMARCA4 gene mutations; iv) patients with complete clinical and pathological data, including sex, age, pathological type, stage, treatment and follow-up information; v) age ≥18 years, with traceable clinical data. The exclusion criteria are as follows: i) Patients with a history of other malignant tumors or who have received other radical treatments for tumors in the past; ii) patients who did not undergo standardized high-throughput sequencing testing or whose sequencing results did not meet the standards; iii) patients with severely missing clinical data that cannot be used for statistical analysis; iv) patients with non-primary lung cancer (such as metastatic cancer). This study focused on analyzing the specific information of *SMARCA4* mutations, including nucleotide variations and amino acid sequence differences. This study was approved by the Ethics Committee of Hunan Provincial People's Hospital (approval no. 2024-279).

Next-generation sequencing experimental methods and instruments. Genomic DNA was extracted from tumor tissue and subjected to next-generation sequencing using probe capture technology, following the procedures described below. First, the extracted genomic DNA was fragmented, and the fragmented DNA was subjected to end repair to blunt the broken ends. Subsequently, an 'A' tail was added to the 3' end of the repaired DNA fragments. After that, sequencing adapters were ligated to the A-tailed DNA fragments, followed by purification to remove unligated adapters and impurities. Next, PCR amplification enrichment was performed using the Pumaikangduo Gene Detection Kit (Nanjing Shihe Gene Biotechnology Co., Ltd.). The PCR products were purified to construct the genomic DNA pre-library. To obtain the targeted library, the pre-library was hybridized and enriched with a DNA probe (cat. no. CM1195; Nanjing Vazyme Biotechnology Co., Ltd.). The quality and integrity of the processed samples (pre-library and targeted library) were verified using a Bioanalyzer 2100 (Agilent Technologies, Inc.), which was used to assess the fragment size distribution and integrity of the libraries; a high-quality library was defined as having a single, sharp peak without obvious smearing, indicating uniform fragment size and good integrity. The concentration of the Equalbit 1x dsDNA HS working solution was measured using a Qubit 4.0 Fluorometer (Thermo Fisher Scientific, Inc.). Library quantification was conducted using the Library Quantification Kit (cat. no. CM1195; Nanjing Vazyme Biotechnology Co., Ltd.), and the final loading concentration of the targeted library was adjusted to 400 pM. The concentration was converted from mass concentration (measured by Qubit 4.0 Fluorometer) to molar concentration using the formula: Molar concentration (pM)=(Mass concentration (ng/μl) x10^6)/(Average library fragment length (bp) x660 g/mol), where the average fragment length of the targeted library was ~300 bp. High-throughput sequencing was performed on the Illumina NextSeq 550Dx sequencing platform (Illumina, Inc.), using paired-end sequencing with a nucleotide length of 150 bp (150 bp per read for both forward and reverse strands). Data analysis was conducted using the built-in BaseSpace Sequence Hub software (version 5.14.0; Illumina, Inc.), which was used for raw data quality control, read alignment, variant calling and data visualization.

Variation annotations and interpretation. The types of driver genes detected can be divided into two categories: i) Driver mutations that promote tumor proliferation and provide selective growth advantages; and ii) passenger mutations with minimal or no impact on tumor proliferation and metastasis (15). Based on the annotation results, genes were evaluated using mutation frequency-based, functional impact-based, structural genomics-based, and network or pathway-based approaches.

Hematoxylin and eosin staining. The tumor tissues used in this study were previously paraffin-embedded and stored after collection. The specific paraffin-embedding process was as follows: Freshly isolated tumor tissues were first fixed to preserve cellular morphology, then dehydrated through a gradient ethanol series, cleared with xylene, embedded in paraffin wax to form tissue blocks, and stored at 4˚C until sectioning (16). Prior to sectioning, the paraffin-embedded tissue blocks were sectioned into slices with a thickness of 4 μm. The histological staining procedures were performed as follows: To remove the paraffin and hydrate the slices, paraffin

slices were sequentially immersed in xylene (twice, 5 min each), followed by anhydrous ethanol (5 min), 95% ethanol (5 min), and 70% ethanol (5 min). Finally, they were washed with distilled water (3 times, 2 min each). The fresh tumor tissues were fixed using 10% neutral buffered formalin (fixative concentration: 10%, v/v) at room temperature (25˚C) for 24 h before paraffin embedding, which was essential to maintain the integrity of tissue structure and cellular components. The sections were then immersed in the hematoxylin staining solution at room temperature (25˚C) for 5 to 10 min. Then, they were differentiated using 0.5% hydrochloric acid-ethanol solution (hydrochloric acid concentration: 0.5%, v/v; ethanol concentration: 70%, v/v) for 30 sec, and 1% ammonia solution (concentration: 1%, v/v) was added dropwise to neutralize the residual acid, thereby making the cell nucleus appear blue-purple. The cytoplasm and matrix were stained pink by immersing the slices in eosin staining solution for 1 to 2 min. After dehydrating the slices in 70% ethanol (5 min), 95% ethanol (5 min), and anhydrous ethanol (twice, 5 min each) in order, they were soaked for 5 to 10 min each in xylene (twice) to attain transparency. After applying neutral gum to the slices and sealing them with a cover glass, the slices were dried in an oven set to 37˚C for 2 h. The stained sections were placed under an Olympus (Olympus Corporation) optical microscope for observation. The cellular and tissue morphological characteristics of smarca4-deficient lung cancer were examined.

Immunohistochemical staining. Immunohistochemical staining was performed following standard protocols. To dewax and hydrate, paraffin slices (4 μm) were successively immersed in xylene (twice, 5 min each, at room temperature, 25˚C) (xylene, analytical grade; Sinopharm Chemical Reagent Co., Ltd.), anhydrous ethanol (5 min, room temperature) (anhydrous ethanol, 99.7% v/v, analytical grade), 95% ethanol (5 min, room temperature) (95% v/v ethanol, prepared by diluting anhydrous ethanol with distilled water), and 70% ethanol (5 min, room temperature) (70% v/v ethanol, prepared by diluting anhydrous ethanol with distilled water). Finally, they were rinsed with PBS buffer (0.01 M, pH 7.4, containing 0.05% Tween-20; Beyotime Biotechnology) three times for 2 min each. Slices were heated to 95˚C in citrate buffer (0.01 M, pH 6.0) using a water bath, held for 15 to 20 min for antigen retrieval (to expose hidden antigen epitopes), allowed to cool naturally to room temperature (~25˚C, ~30 min), and rinsed with PBS buffer (0.01 M, pH 7.4, 0.05% Tween-20) three times, for 2 min each. After 10 to 20 min of sealing the slices with a sealing solution [5% BSA (cat. no. A7906; MillaporeSigma) dissolved in PBS buffer, 0.01 M, pH 7.4] at room temperature to prevent non-specific binding, the primary antibody (anti-Ki-67 rabbit monoclonal antibody; cat. no. ab15580; 1:100; Abcam) was applied dropwise (50 μl per slice, covering the entire tissue section) and incubated overnight at 4˚C. The slices were washed with PBS buffer (0.01 M, pH 7.4, 0.05% Tween-20) three times, 5 min each, to remove unbound primary antibody. The secondary antibody (goat anti-rabbit IgG H&L HRP; cat. no. ab6721; 1:200; Abcam) was applied dropwise (50 μl per slice) and incubated at 37˚C for 30 to 60 min. Next, the DAB solution (Dako; Agilent Technologies, Inc.) was applied dropwise (50 μl per slice), and the slices were observed under a light microscope (Olympus BX53; Olympus Corporation) at x100 magnification to monitor the color development. After 5 to 10 min (until the positive signal showed a light brown color, avoiding over-coloration), the reaction was stopped with distilled water (room temperature) by rinsing three times, 1 min each, and hematoxylin (cat. no. C0107; Beyotime Biotechnology) was used as a light counterstain for the cell nucleus (stained at room temperature for 30 sec). Slices were dehydrated using 70% ethanol (5 min, room temperature), 95% ethanol (5 min, room temperature) and anhydrous ethanol (twice, 5 min each, room temperature) in order, and xylene (twice, 5 min each, room temperature) was used to make them transparent. Finally, a neutral gum (Sinopharm Chemical Reagent Co., Ltd.) was applied dropwise (3-5 μl per slice) for sealing, and the slices were dried at 37˚C in an oven for 2 h before microscopic observation.

Gene Expression Profiling Interactive Analysis (GEPIA)2. GEPIA2 (http://gepia2.cancer-pku.cn/) is an online tool for gene expression analysis based on the TCGA and GTEx databases. In the present study, GEPIA2 was used to analyze the differential expression of target genes between tumor and normal tissues. The corresponding cancer dataset was selected, with tumor tissues as the experimental group and normal tissues as the control group, and box plots were used to display the expression distribution. In the survival analysis module, patients were divided into high- and low-expression groups using the median expression value as the cut-off. Survival curves were plotted by the Kaplan-Meier method, and survival differences were evaluated using the Log-rank test. In addition, the correlation analysis module was applied to explore the expression correlation between genes using Pearson correlation coefficient to screen co-expressed genes. $P<0.05$ was considered to indicate a statistically significant difference.

Statistical analysis. All experimental data were presented as mean ± standard deviation and each experiment was independently repeated three times to ensure the reliability and reproducibility of the experimental results. Statistical tests were selected based on the experimental design: Unpaired two-tailed t-test was used for comparison between two independent groups, while one-way analysis of variance followed by Tukey's post-hoc test was employed for multiple group comparisons. All statistical analyses were performed using SPSS software (version 26.0; IBM Corp.). $P<0.05$ was considered to indicate a statistically significant difference.

Results

Clinical and pathological characteristics of SMARCA4-dNSCLC. Between January 2021 and November 2024, 15 patients with NSCLC and *SMARCA4* mutations were identified. All the 15 patients in this study were from Hunan Province, China, and were diagnosed with *SMARCA4*-deficient NSCLC by pathological examination. The likelihood of lung cancer developing in the left and right lungs was equal, and there was no discernible pattern in the location of cases. In general, the tumor was large, measuring >5 cm in diameter. The symptoms of *SMARCA4*-deficient NSCLC are consistent with those of common NSCLC (such as cough and chest pain), but due to

Table I. Clinical characteristics of *SMARCA4*-deficient non-small cell lung cancer.

Patient no.	Sex	Age, years	Tumor location (left or right lung)	TNM staging[a]	Differentiation	Tumor size, cm	Treatment
1	Female	76	Left	T3AN0M0	Low	6.21x3.43x4.50	IM
2	Male	65	Left	T2bN0M0	Low	5.32x4.29x1.54	S + CM
3	Female	84	Left	T4bN0M1	Low	4.45x4.47x3.22	P
4	Female	47	Left	T4N0M1	Low	10.04x6.28x6.28	CM + TR
5	Male	72	Left	T2bN3M1b	Low	4.64x4.52x4.25	IM
6	Female	69	Left	T2aN2M1	Low	5.32x5.46x3.52	TR + R
7	Male	51	Left	T4N0M0	Low	6.49x5.00x2.21	S
8	Male	64	Right	T4NxM1	Undifferentiated	7.00x4.70x4.21	IM
9	Female	34	Right	T2bN0M0	Low	5.33x4.12x1.57	CM +IM
10	Male	50	Right	T2bN0M0	Low	2.23x1.82x1.62	S
11	Male	72	Right	T4N0M1b	Undifferentiated	3.51x3.41x1.80	IM
12	Male	56	Right	T4N3M1	Low	3.21x3.21x2.20	CM
13	Male	66	Right	T4NxM0	Undifferentiated	4.54x4.45x1.53	CM +IM
14	Female	59	Right	T2bN0M0	Low	5.20x3.40x2.54	CM + TR
15	Male	43	Right	T3N1bM1	Moderately	6.22x4.18x3.54	P

[a]TNM Staging (version 9th) from IASLC Thoracic Oncology Staging Manual (28). IM, immunotherapy; S, surgery; CM, chemotherapy; TR, target therapy; R, radiation therapy; P, palliative therapy.

tumor growth characteristics (some reports suggest strong invasiveness), some symptoms may be more pronounced or appear earlier. Any other prominent characteristic co-morbidities had not been found in the 15 patients studied. Additionally, surgery combined with immunotherapy or targeted therapy was the primary treatment (Table I). Microscopic examination showed map-shaped necrosis and cancer cells arranged in a patchy, island-shaped or acinar pattern. Tumor cells appeared as small epithelioid cells; some had abundant cytoplasm, eosinophilic or translucent nuclei, vacuolated nuclei, distinct nucleoli, and visible mitotic figures (Fig. 1A-C). Strong tumor proliferation was observed in ~50% of the regions with Ki67-positive expression (Fig. 1D). The staining results showed that the normal bronchial and alveolar epithelial cells were positive for the epithelial markers CK7, NapsinA and TTF-1 (Fig. 1E-G), while the tumor tissues did not express these proteins. Both the squamous epithelial markers P63 and P40 showed positive basement membrane and negative tumor tissue (Fig. 1H and I). The two neuroendocrine markers, Syn and CD56, showed a pattern of weakly positive and negative expression, respectively, in the tumor tissues (Fig. 1J and K). Tumor cells showed a high level of the mesenchymal marker Vimentin (Fig. 1L). Overall, 15 cases of *SMARCA4*-deficient non-small cell lung cancer were characterized by large tumor size and high invasiveness, with prominent geographic necrosis and epithelioid cell morphology histologically, and an immunophenotype featuring negative epithelial markers and high expression of the mesenchymal marker Vimentin.

Expression of biomarkers related to targeted immunotherapy in SMARCA4-dNSCLC. Comparison of the immunohistochemical expression characteristics of EGFR, anaplastic lymphoma kinase (ALK) (D5H3), P53 and programmed cell death 1 ligand 1 (PD-L1) in 15 patients with *SMARCA4*-deficient tumors showed that the EGFR protein could be either expressed positively (3/15) (Fig. 2A and I) or negatively (12/15) (Fig. 2B and I) in *SMARCA4*-deficient tumors. However, cases of ALK protein expression (D5H3) positivity in *SMARCA4*-deficient tumors were lacking (Fig. 2E and I). Additionally, the PD-L1 protein (4/15) had a low likelihood of positivity, as it was only expressed in 4/15 patients (Fig. 2C and I), whereas it was negatively expressed in 11/15 patients (Fig. 2D and I). Furthermore, compared with the wild-type protein expression of P53, the P53 protein showed a higher likelihood of exhibiting complete negative (4/14) or complete positive mutations (11/15), because the P53 protein has three expression patterns, partial positivity indicates the wild type, while complete negativity or complete positivity indicates the mutant type (Fig. 2F-H and J). In SMARCA4-deficient NSCLC, EGFR, ALK, and PD-L1 positivity rates were low, while P53 showed a high frequency of aberrant expression, suggesting limited benefit from conventional targeted therapy and a potential subtype-specific molecular profile.

SMARCA4 mutation situation in NSCLC. The spectrum of gene mutations in 15 *SMARCA4*-deficient patients with lung cancer were summarized in Table II. Patients 4 and 12 shared the same mutation type, c.2729C>T (p.T910M). The genetic mutation types of patient 7 and patient 8 are the same; both have experienced a copy number deletion. Furthermore, patient 13 was unique: Three mutations were detected in *SMARCA4* of this patient, namely c.3634_3636del (p. E1212del), c.3574C>T (p.R1192C), and c.3733G>A (p.A1245T) (Fig. 3A). SMARCA4 encodes the BRG1 protein, while SMARCB1 encodes the INI1 protein. In clinical diagnosis, immunohistochemical pairing is frequently used to screen for BRG1 and

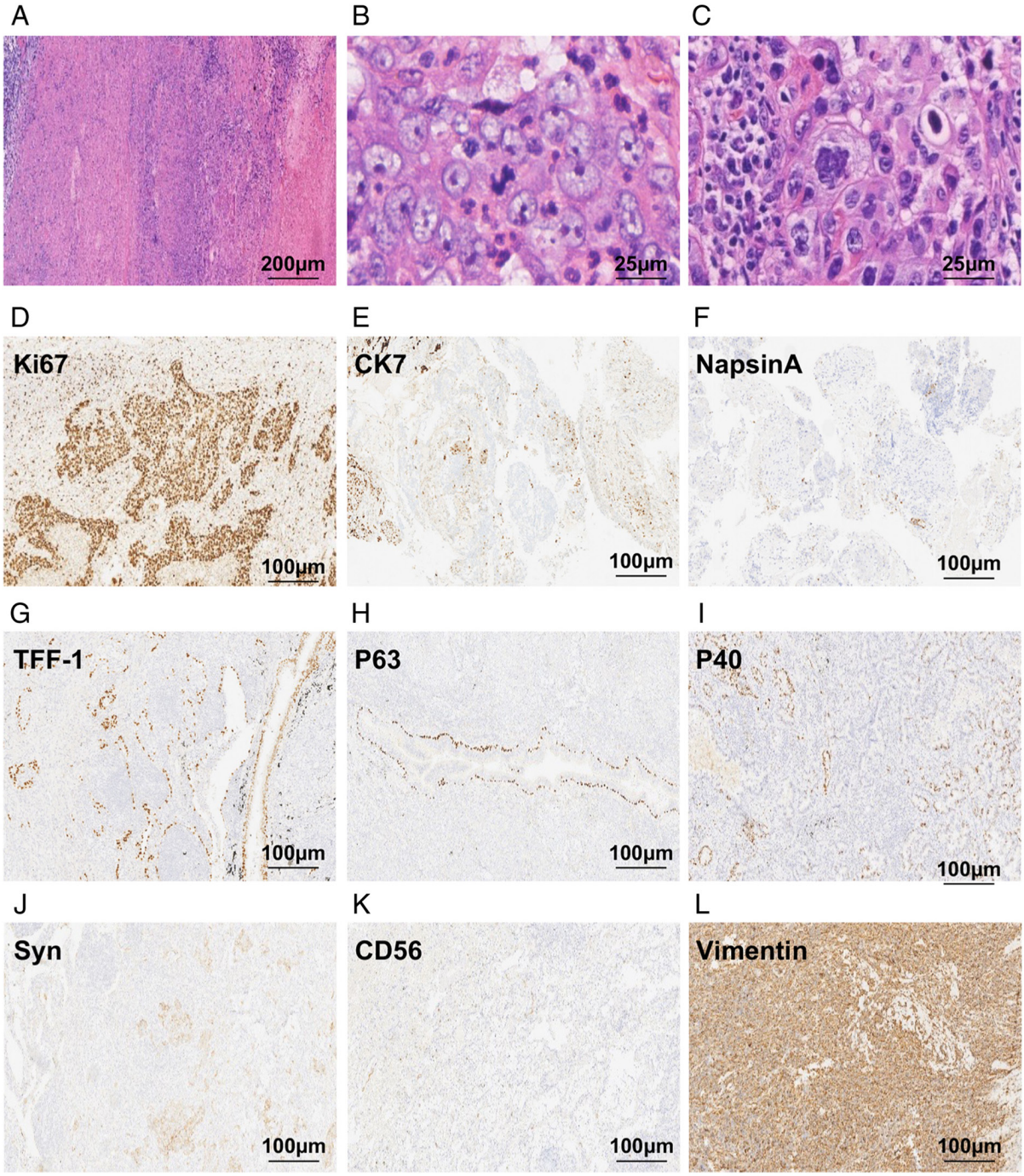

Figure 1. H&E staining and diagnostic immunohistochemical staining of lung cancer tissues. (A) H&E staining shows that the tumor cells were solid and distributed in patches, with a large number of tumor cells and a diffuse distribution (scale bar, 200 μm). (B) The tumor cells are vesicular in shape, large in size and the cytoplasm is lightly stained (scale bar, 25 μm). (C) H&E staining shows that a poorly differentiated tumor with singular nuclei and large tumor cells with giant nuclei in *SMARCA4*-dNSCLC cases (scale bar, 25 μm). (D) Ki67 expression shows 50% positivity (scale bar, 100 μm). Adeno-epithelial markers (scale bar, 100 μm). (E) CK7, (F) NapsinA and (G) TTF-1 show positivity in bronchial and alveolar epithelium, whereas tumor tissue shows negativity (scale bar, 100 μm). Both squamous epithelial markers (H) P63 and (I) P40 show positive basement membrane and negative tumor tissue (scale bar, 100 μm). Neuroendocrine markers (J) Syn and (K) CD56 show weak positivity or negativity (scale bar, 100 μm). (L) The mesenchymal marker Vimentin shows strong positivity in tumor cells (scale bar, 100μm). H&E, hematoxylin and eosin; dNSCLC, deficient non-small cell lung cancer; Syn, synaptophysin; TTF-1, thyroid transcription factor-1.

INI1 protein expression to detect SMARCA4-deficient lung cancer. The BRG1 protein encoded by the SMARCA4 was not expressed (the BRG1-stained positive areas in Fig. 3B are normal alveolar epithelium, not tumor regions), whereas the INI1 protein expression was partially positive (6/15) (Fig. 3B). Additionally, IHC was conducted on the tumor tissues of the 15 patients with *SMARCA4*-deficient lung cancer. Some patients showed negative INI1 expression, as shown in the left part of Fig. 3C, while some showed positive expression, as shown in the right part of Fig. 3C. Only patients 1, 5, 6, 13, 14 and 15 showed positive INI1 protein expression, whereas the remaining nine patients showed negative expression. Table II

Table II. Mutation situation of *SMARCA4* in non-small cell lung cancer and the expression of INI1.

Patient no.	Mutation location	INI1 expression
1	c.3607C>T (p.R1203C)	Positive
2	c.3663G>T (p.K1221N)	Negative
3	c.4053del (p. D1351Efs*7)	Negative
4	c.2729C>T (p.T910M)	Negative
5	c.1245+577_1348del	Positive
6	c.2799C>G (p.F933L)	Positive
7	c.2342T>C (p.M781T), CNV=1	Negative
8	c.2439-1G>A, CNV=1	Negative
9	c.2342T>C (p.M781T)	Negative
10	IGR (upstream TIMM29) ~SMARCA4: exon16	Negative
11	c.2439-1G>A	Negative
12	c.2729C>T (p.T910M)	Negative
13	c.3634_3636del (p. E1212del); c.3574C>T (p.R1192C); c.3733G>A (p.A1245T)	Positive
14	c.2942A>G (p.K981R)	Positive
15	c.3580G>A (p.G1194R)	Positive

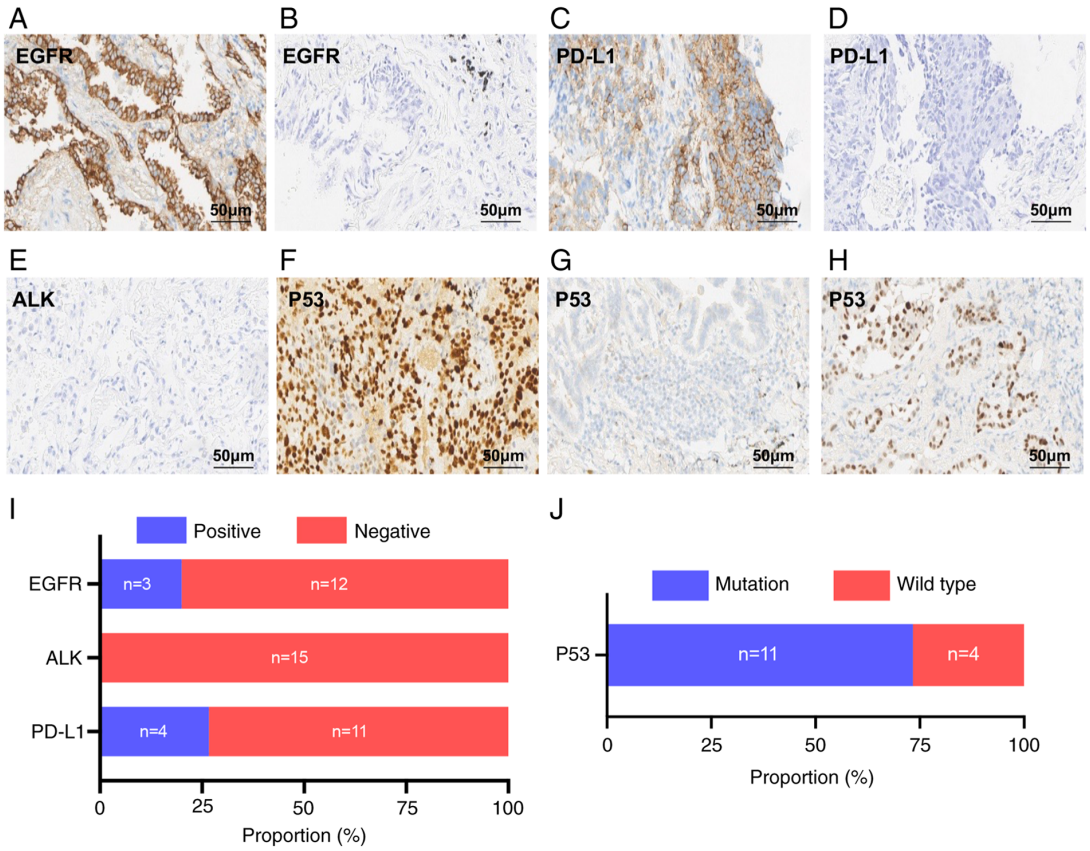

Figure 2. Immunohistochemical staining of EGFR, PD-L1, ALK and P53 in lung cancer tissue. (A) EGFR shows positively-stained cancer cells. (B) EGFR shows negative-stained cancer cells. (C) PD-L1 shows positively-stained cancer cells. (D) PD-L1 shows negatively-stained cancer cells. (E) ALK shows negatively-stained cancer cells. (F) P53 shows positively-stained cancer cells. (G) P53 shows negatively-stained cancer cells. (H) P53 shows positively-stained cancer cells. Scale bar, 50 μm. (I) The proportion of negative and positive staining of EGFR, PD-L1 and ALK. (J) The proportion of mutated and wild-type P53. PD-L1, programmed cell death 1 ligand 1; ALK, anaplastic lymphoma kinase.

shows the representative expression of the INI1 protein, along with the corresponding mutation profile. Among the 15 *SMARCA4*-deficient patients with NSCLC, diverse mutations including missense, copy number loss, and multiple concurrent variants were detected, with loss of BRG1 expression and heterogeneous INI1 expression, supporting the value of IHC

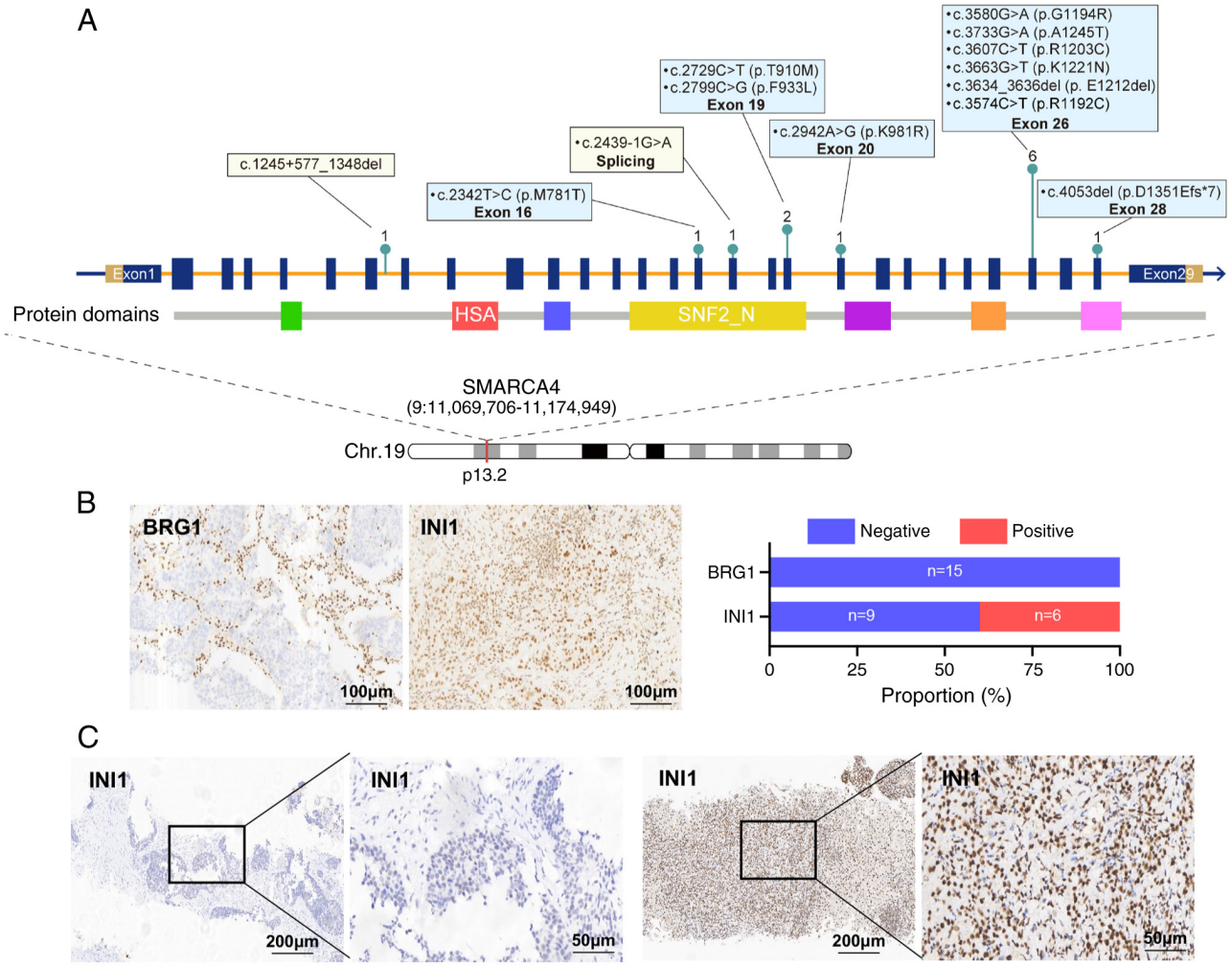

Figure 3. *SMARCA4* mutation in patients with *SMARCA4*-dNSCLC. (A) The *SMARCA4* mutation site in 15 patients with *SMARCA4*-dNSCLC. (B) The proportion of negative and positive staining of BRG1 and INI1 (scale bar, 100 μm). (C) Representative images of negative and positive staining of INI1 (left images scale bars, 200 μm; right images scale bars, 50 μm). dNSCLC, deficient non-small cell lung cancer; BRG1, BOI-related E3 ubiquitin-protein ligase 1; HSA, *Homo sapiens*.

pairing of BRG1 and INI1 in the clinical identification of this molecular subtype.

Characteristics of gene mutations in SMARCA4-dNSCLC. The gene mutation profiles of 15 patients were analyzed. *NQO1* and *TP53* mutations were detected in nine patients, *XRCC1* mutation was detected in seven, *DPYD* mutation was detected in six, *TYMS* mutation was detected in five, *GSTP1*, *MTHFR*, *LRP1B* and *UGT1A1* mutations were detected in four, and *GSTT1*, *GSTM1*, *ID3*, *ERCC1*, *ERCC2*, *ARID1A*, *RAD54L* and *TERT* mutations were detected in three (Fig. 4A). All mutated genes are shown in Table SI. The enrichment analysis conducted on the identified gene set using the Gene Expression Profiling Interactive Analysis (GEPIA)2 database revealed the presence of mutated genes such as 'EGFR tyrosine kinase inhibitor resistance', 'non-small cell lung cancer', 'ErbB signaling pathway', 'protein kinase regulator activity', 'extrinsic apoptotic signaling pathway' and 'regulation of ERK1 and ERK2 cascade'. The same pathway demonstrated significant enrichment (Fig. 4B). Additionally, the 15 patients with lung cancer and *SMARCA4* deficiency demonstrated partial mutations of specific genes. For example, *NQO1* c.559C>T (p.P187S) and *XRCC1* c.1196A>G (p.Q399R) were detected 7 times, *DPYD* c.1627A>G (p.I543V) was detected 5 times, and *TYMS* c.*450_*455delAAGTTA, *GSTP1* c.313A>G (p.I105V) and *MTHFR* c.665C>T (p.A222V) were detected 4 times. These three gene loci exhibited four different mutations (Table III). The high-frequency mutation genes and sites may control the incidence and progression of *SMARCA4*-deficient lung cancer. These results identified a distinct mutation spectrum involving DNA repair, metabolic and cancer-related genes in *SMARCA4*-deficient NSCLC, with several recurrent high-frequency mutation sites that may contribute to tumorigenesis and progression via pathways closely associated with NSCLC and therapy resistance.

Discussion

The present study used second-generation sequencing technology to analyze the characteristics of molecular, immunohistochemical and morphological mutations in 15 cases of *SMARCA4*-dNSCLC. Although the expression of the BRG1 protein encoded by *SMARCA4* was low, the expression of the INI1 protein encoded by *SMARCB1* was primarily

Table III. Mutation site and frequency of genes in patients with *SMARCA4*-deficient non-small cell lung cancer.

Gene name	Mutation site
NQO1	c.559C>T (p.P187S) (n=7); c.415C>T (p.R139W) (n=2)
TP53	L194R exon6 SNV (n=1); c.258_261dup (p.A88Tfs*62) (n=1); c.876dup (p.G293Rfs*13) (n=1); c.514G>T (p.V172F) (n=1); c.489C>A (p.Y163*) (n=1); c.488A>G (p.Y163C) 18.2% 15.4% (n=1); c.818G>A p.R273H exon8 33.23% (n=1); c.949C>T p.Q317* exon9 52.22% (n=1); c.461G>T (p.G154V) 0.63% 40.28% (n=1)
XRCC1	XRCC1 c.1196A>G (p.Q399R) (n=7)
DPYD	c.1627A>G (p.I543V) (n=5); c.2194G>A (p.V732I) (n=1)
TYMS	c.-97_70CCGCGCCACTTGGCCTGCCTCCGTCCCG (n=1); c.*450_*455delAAGTTA (n=4),
GSTP1	c.313A>G (p.I105V) (n=4)
MTHFR	c.665C>T (p.A222V) (n=4)
UGT1A1	c.-55_-54insAT (n=3); c.211G>A (p.G71R) (n=1)
LRP1B	c.9644C>A (p.P3215Q) (n=1); c.5018C>T (p.T1673M) (n=1); c.3910T>A (p.W1304R) (n=1); c.11539G>T p.E3847* (n=1)
GSTT1	Homozygous deletion polymorphism of GSTT1 (n=3)
GSTM1	Homozygous deletion polymorphism of GSTM1 (n=3)
ID3	c.208C>G p.L70V (n=1), c.241C>T p.Q81* (n=1); c.309_312del p. T105Rfs*20 (n=1)
ERCC1	c.354T>C (p. N118) (n=3)
ERCC2	c.2251A>C (p.K751Q) (n=3)
ARID1A	c.5769del (p. F1924Sfs*59) (n=1); c.827del (p. G276Efs*87) (n=1); c.3218G>A p.W1073* (n=1)
RAD54L	c.1258C>A (p.Q420K) (n=1); c.1337C>T (p.S446F) (n=2)
TERT	c.1647G>A (p.M549I) (n=1); c.-124C>T-promoter (n=1); Copy number amplification CN:4.9 (n=1)

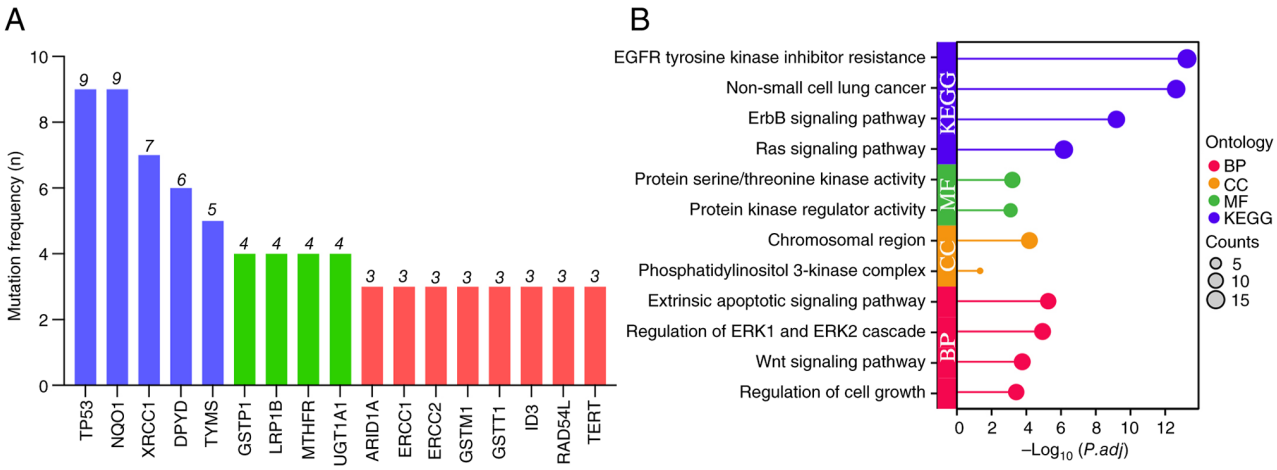

Figure 4. Characteristics of gene mutations in *SMARCA4*-deficient lung cancer. (A) Genes with a mutation frequency ≥3 in 15 patients with *SMARCA4*-dNSCLC. (B) Enrichment analysis of all mutated genes in 15 patients with *SMARCA4*-dNSCLC. dNSCLC, deficient non-small cell lung cancer.

positive. This finding provided evidence for the diagnosis of *SMARCA4*-dNSCLC. Additionally, immunohistochemical characteristics, such as CK7 negativity, NapsinA positivity, TTF-1 and Vimentin positivity, further support the diagnosis of *SMARCA4*-deficient NSCLC. According to immunohistochemical expression characteristics, *SMARCA4*-deficient NSCLC can exhibit both positive and negative expression of the EGFR protein; however, most cases were negative. Thus, *SMARCA4* deficiency may not be associated with the status of the EGFR mutation. In SMARCA4 deficiency-type tumor tissues, NapsinA and TTF-1 are not expressed. These immunohistochemical markers are only expressed in the local normal epithelial tissues adjacent to the tumor tissues. *P53* mutations may be more prevalent in *SMARCA4*-deficient NSCLC, as evidenced by the increased likelihood of complete negative or positive mutations in the P53 protein, compared with wild-type P53 protein expression types. However, the efficacy of immunotherapy may be impacted by the low likelihood of positive PD-L1 protein. Notably, although the present study did not identify any cases of ALK (D5H3) protein positivity in *SMARCA4*-dNSCLC, the small sample size prevents us from concluding whether *SMARCA4* and *ALK* mutations are mutually exclusive. In the future, we hope to accumulate more cases to fully study this issue.

The *SMARCA4* mutation is strongly associated with lung cancer, particularly NSCLC and large cell carcinoma (LCC) (15). Overall, ~10% of NSCLC cases have *SMARCA4* mutations, and ~50% of these tumors exhibit typical smoking-related co-mutations. Among the 15 patients, 9 were male and all of them had a history of smoking (17). Notably, compared with other histological tumor subtypes, LCC has a higher frequency of *SMARCA4* mutations. Of all LCCs, 40.5% are *SMARCA4*-deficient, whereas 51.4% are *SMARCA4*-mutant tumors (18). These mutations substantially affect patient prognosis, and the *SMARCA4* mutation has emerged as a biomarker for poor prognosis in lung cancer. Additionally, it has a predictive value in cancer treatment (19). *SMARCA4* mutations or their abnormalities are mutually exclusive with EGFR mutations and are associated with a history of smoking and poor prognosis, and are mutually exclusive with *EGFR* mutations (7,20). A previous multivariate analysis confirmed that the *SMARCA4* mutation is an independent prognostic factor for lung cancer.

At present, to the best of our knowledge, there is no established criterion for determining the responsiveness of *SMARCA4* mutations to a targeted therapy approach. However, *SMARCA4* mutant tumors are more likely to have mutations in KRAS, serine/threonine kinase 11 and Kelch-like ECH-related protein 1 (21). These combined mutations may affect treatment responsiveness, which will lead to even poorer treatment outcomes for the patients. In addition, patients with mutations in the SMARCA4 gene have a poorer response to immunotherapy; however, further research is warranted to determine the specific mechanisms and treatment strategies. It has been reported in the literature that the interactions between SMARCA4 and members of the SMARC, ARID and H3C families may be associated with cellular telomere and telomerase activities (22). The PD-L1 expression level of tumors, tumor mutation burden (TMB), and the overall health of the patient are typically considered when determining whether patients with lung cancer are candidates for immunotherapy (23). Patients with *SMARCA4*-deficient lung cancer are more likely to benefit from immunotherapy because they have a higher PD-L1 positive expression rate and a relatively high TMB. Additionally, in line with previous studies, *SMARCA4* mutations are mutually exclusive with common driver gene mutations, such as EGFR, anaplastic lymphoma kinase, and ROS1 (24). However, given the small sample size of the present study, the mutation frequency is not representative and there is need for more studies with larger multi-center cohorts to confirm these findings.

SMARCA4 mutations affect lung cancer treatment by affecting the patient's responsiveness to immunotherapy (for example, PD-1 and PDL-1). *SMARCA4*-deficient tumors frequently exhibit highly undifferentiated pathological features, particularly in large cell carcinoma, where the deficiency occurs in ~50% of cases. Combination therapy with immunotherapy is the first-line treatment for patients with *SMARCA4*-deficient lung cancer. However, the efficacy of single immunotherapy may be insufficient; thus, the combination of chemotherapy and anti-angiogenic drugs can markedly improve the progression-free survival (25). Particularly, anti-angiogenic drugs, such as bevacizumab, can be used in conjunction with immunotherapy to further reduce tumor angiogenesis and delay disease progression. Programmed cell death protein 1 (PD-1) and PD-L1 inhibitors have comparable overall effects in NSCLC; nonetheless, in some cases, PD-1 inhibitors may be moderately more effective. As *SMARCA4*-deficient NSCLC is associated with a highly malignant type of lung cancer, we found that most patients were no longer able to receive follow-up and consultation when collecting data, so we were unable to obtain more detailed treatment plans in this cohort of 15 patients (26,27). However, the adverse effects of PD-L1 inhibitors are relatively mild; thus, doctors can select the most suitable course of treatment for each patient based on their specific circumstances.

Although the present study has achieved some notable results, there are still some issues that need to be further explored, which is also the direction for future research. This study had a limited sample size of only 15 patients with *SMARCA4*-deficient lung cancer. In the future, large-scale cohort validation is needed to investigate more characteristics of *SMARCA4*-deficient lung cancer and elucidate the relationship between *SMARCA4* mutations and other gene mutations (such as *NQO1, P53* and *ALK*) and how they affect the response to immune therapy. Additionally, further research and clinical trial validation are required for targeted therapeutic strategies for *SMARCA4*-deficient NSCLC.

In conclusion, this study provided information for the diagnosis and treatment of *SMARCA4*-deficient NSCLC by systematically analyzing its clinical and pathological features, immunohistochemical expression characteristics, and molecular pathways.

Acknowledgements

Not applicable.

Funding

This work was financially supported by the Youth Doctoral Fund Project of Hunan Provincial People's Hospital (grant no. BSJJ202218) and Natural Science Foundation of Hunan Province (grant no. 2025JJ60591).

Availability of data and materials

The raw sequence data reported in this paper have been deposited in the Genome Sequence Archive (Genomics, Proteomics & Bioinformatics 2025) in National Genomics Data Center, Chinese Academy of Sciences that are publicly accessible at https://ngdc.cncb.ac.cn/gsa-human/browse/HRA016167 (bioproject no. PRJCA055910).

Authors' contribution

FY and YS designed the entire scientific experiment and all the data collection, conducted the genetic testing experiment, and also participated in the writing of the main part of the paper. ZC and YL contributed to the diagnosis and analyzed the results. YY contributed to collecting clinical data. FY and YS revised the final manuscript. All authors read and approved the final manuscript. FY and YS confirm the authenticity of all the raw data.

Ethics approval and consent to participate

Written informed consent was obtained from each patient to participate in this study. This study was approved by the Ethics Committee of the Hunan Provincial People's Hospital (approval no. 2024-279).

Patient consent for publication

Each patient provided consent for their information to be published.

Competing interests

The authors declare that they have no competing interests.

References

1. Tian Y, Xu L, Li X, Li H and Zhao M: SMARCA4: Current status and future perspectives in non-small-cell lung cancer. Cancer Lett 554: 216022, 2023.
2. Witkowski L, Nichols KE, Jongmans M, van Engelen N, de Krijger RR, Herrera-Mullar J, Tytgat L, Bahrami A, Mar Fan H, Davidson AL, *et al*: Germline pathogenic SMARCA4 variants in neuroblastoma. J Med Genet 60: 987-992, 2023.
3. Qiu Z and Ghosh A: A calcium-dependent switch in a CREST-BRG1 complex regulates activity-dependent gene expression. Neuron 60: 775-787, 2008.
4. Wang T, Peng B, Luo T, Tian D, Zhao Z, Fu Z and Li Q: ZEB1 recruits BRG1 to regulate airway remodelling epithelial-to-mesenchymal transition in asthma. Exp Physiol 107: 515-526, 2022.
5. Katayama Y, Iwasaki T, Yamamoto T, Shimada N, Nakashima M, Toya M, Narutomi F, Tomonaga T, Kato K and Oda Y: Loss of SMARCA4 induces sarcomatogenesis through epithelial-mesenchymal transition in ovarian carcinosarcoma. Cancer Sci 116: 835-845, 2025.
6. Duplaquet L, So K, Ying AW, Pal Choudhuri S, Li X, Xu GD, Li Y, Qiu X, Li R, Singh S, *et al*: Mammalian SWI/SNF complex activity regulates POU2F3 and constitutes a targetable dependency in small cell lung cancer. Cancer Cell 42: 1352-1369.e13, 2024.
7. Pang LL, Zhou HQ, Zhang YX, Zhuang WT, Pang F, Chen LJ, Liao J, Huang YH, Mao TQ, Mai ZH, *et al*: SWI/SNF family mutations in advanced NSCLC: genetic characteristics and immune checkpoint inhibitors' therapeutic implication. ESMO Open 9: 103472, 2024.
8. Malone HA and Roberts CWM: Chromatin remodellers as therapeutic targets. Nat Rev Drug Discov 23: 661-681, 2024.
9. Radko-Juettner S, Yue H, Myers JA, Carter RD, Robertson AN, Mittal P, Zhu Z, Hansen BS, Donovan KA, Hunkeler M, *et al*: Targeting DCAF5 suppresses SMARCB1-mutant cancer by stabilizing SWI/SNF. Nature 629: E12, 2024.
10. Jang JY, Seo JH, Choi JJ, Ryu HJ, Yun H, Ha DM and Yang J: Insight into microbial extracellular vesicles as key communication materials and their clinical implications for lung cancer (Review). Int J Mol Med 56: 119, 2025.
11. Li Q, Zhang Z, Wang Y, Peng X, Fang Y, Zhang Y, Chen L, Huang T, Yang Z, Li C, *et al*: ARID1A Mediates SWI/SNF-independent maintenance of heterochromatin architecture to restrain viral mimicry and immunogenicity in colon cancer. Cancer Res 2026 (Epub ahead of print).
12. Shi M, Pang L, Zhou H, Mo S, Sheng J, Zhang Y, Liu J, Sun D, Gong L, Wang J, *et al*: Rare SMARCA4-deficient thoracic tumor: Insights into molecular characterization and optimal therapeutics methods. Lung Cancer 192: 107818, 2024.
13. Qiu X, You L, Wang C and Sheng J: Non small cell lung cancer with SMARCA4 deficiency harboring rare EGFR mutations exhibited significant tumor response when treated with afatinib: A case report. Front Med 19: 170-173, 2025.
14. Yavas A, Ozcan K, Adsay NV, Balci S, Tarcan ZC, Hechtman JF, Luchini C, Scarpa A, Lawlor RT, Mafficini A, *et al*: SWI/SNF complex-deficient undifferentiated carcinoma of the pancreas: Clinicopathologic and genomic analysis. Mod Pathol 37: 100585, 2024.
15. Zane LK, Yee LM, Chang TC, Sklar J, Yang G, Wen JD, Li P, Harrington R, Sims DJ, Harper K, *et al*: A concordance study among 26 NGS laboratories participating in the NCI molecular analysis for therapy choice clinical trial. Clin Cancer Res 31: 3512-3525, 2025.
16. Hötzel KJ, Havnar CA, Ngu HV, Rost S, Liu SD, Rangell LK and Peale FV: Synthetic Antigen Gels as Practical Controls for Standardized and Quantitative Immunohistochemistry. J Histochem Cytochem 67: 309-334, 2019.
17. Longo V, Catino A, Montrone M, Montagna ES, Pesola F, Marech I, Pizzutilo P, Nardone A, Perrone A, Gesualdo M and Galetta D: Treatment of thoracic SMARCA4-deficient undifferentiated tumors: Where we are and where we will go. Int J Mol Sci 25: 3237, 2024.
18. Miyazaki N, Ibusuki A, Higashi Y, Yoshizaki A, Miyauchi I, Sakaguchi I, Kitazono I, Egawa G and Kanekura T: Thoracic SMARCA4-deficient undifferentiated tumor diagnosed from a rapidly enlarging cutaneous metastasis. J Dermatol 53: e238-e239, 2026.
19. Deng Q, Lakra P, Gou P, Yang H, Meydan C, Teater M, Chin C, Zhang W, Dinh T, Hussein U, *et al*: SMARCA4 is a haploinsufficient B cell lymphoma tumor suppressor that fine-tunes centrocyte cell fate decisions. Cancer Cell 42: 605-622.e11, 2024.
20. Wei XW, Lu C, Zhang YC, Fan X, Xu CR, Chen ZH, Wang F, Yang XR, Deng JY, Yang MY, *et al*: Redoxhigh phenotype mediated by KEAP1/STK11/SMARCA4/NRF2 mutations diminishes tissue-resident memory CD8+ T cells and attenuates the efficacy of immunotherapy in lung adenocarcinoma. Oncoimmunology 13: 2340154, 2024.
21. De Giglio A, De Biase D, Favorito V, Maloberti T, Di Federico A, Zacchini F, Venturi G, Parisi C, Gustavo Dall'Olio F, Ricciotti I, *et al*: STK11 mutations correlate with poor prognosis for advanced NSCLC treated with first-line immunotherapy or chemo-immunotherapy according to KRAS, TP53, KEAP1, and SMARCA4 status. Lung Cancer 199: 108058, 2025.
22. Zhang H, Pandey S, Travers M, Sun H, Morton G, Madzo J, Chung W, Khowsathit J, Perez-Leal O, Barrero CA, *et al*: Targeting CDK9 reactivates epigenetically silenced genes in cancer. Cell 175: 1244-1258.e26, 2018.
23. Alessi JV, Elkrief A, Ricciuti B, Wang X, Cortellini A, Vaz VR, Lamberti G, Frias RL, Venkatraman D, Fulgenzi CAM, *et al*: Clinicopathologic and genomic factors impacting efficacy of first-line chemoimmunotherapy in advanced NSCLC. J Thorac Oncol 18: 731-743, 2023.
24. Nambirajan A, Singh V, Bhardwaj N, Mittal S, Kumar S and Jain D: SMARCA4/BRG1-deficient non-small cell lung carcinomas: A case series and review of the literature. Arch Pathol Lab Med 145: 90-98, 2021.
25. Kawachi H, Kunimasa K, Kukita Y, Nakamura H, Honma K, Kawamura T, Inoue T, Tamiya M, Kuhara H, Nishino K, *et al*: Atezolizumab with bevacizumab, paclitaxel and carboplatin was effective for patients with SMARCA4-deficient thoracic sarcoma. Immunotherapy 13: 799-806, 2021.
26. Sun F, Zou B, Li H, Xu C, Luo Q, Wang C, Xu P, Pei D, Chen J, Qin D, *et al*: Structural basis for BCL7B-mediated ncBAF-nucleosome engagement. Nucleic Acids Res 54: gkag092, 2026.
27. Liu Y, Li H, Li X, Cui H, Li R, Zhu J, Cui H, Liu Y and Cheng Y: Clinicopathological characteristics and therapeutic outcomes in patients with non-small cell lung cancer harboring SMARCA4 mutations. Ann Med 58: 2620201, 2026.
28. Rami-Porta R, Nishimura KK, Giroux DJ, Detterbeck F, Cardillo G, Edwards JG, Fong KM, Giuliani M, Huang J, Kernstine KH Sr, *et al*: The International Association for the Study of Lung Cancer lung cancer staging project: Proposals for revision of the TNM stage groups in the forthcoming (Ninth) Edition of the TNM classification for lung cancer. J Thorac Oncol 19: 1007-1027, 2024.